JHEP

Published for SISSA by Springer

Received: August 22, 2016
Accepted: October 17, 2016
Published: October 26, 2016

Homes' law in holographic superconductor with Q-lattices

Chao Niu and Keun-Young Kim

School of Physics and Chemistry, Gwangju Institute of Science and Technology, Gwangju 61005, Korea

E-mail: chaoniu09@gmail.com, fortoe@gist.ac.kr

Abstract: Homes' law, $\rho_s = C\sigma_{\rm DC}T_c$, is an empirical law satisfied by various superconductors with a material independent universal constant C, where ρ_s is the superfluid density at zero temperature, T_c is the critical temperature, and $\sigma_{\rm DC}$ is the electric DC conductivity in the normal state close to T_c. We study Homes' law in holographic superconductor with Q-lattices and find that Homes' law is realized for some parameter regime in insulating phase near the metal-insulator transition boundary, where momentum relaxation is strong. In computing the superfluid density, we employ two methods: one is related to the infinite DC conductivity and the other is related to the magnetic penetration depth. With finite momentum relaxation both yield the same results, while without momentum relaxation only the latter gives the superfluid density correctly because the former has a spurious contribution from the infinite DC conductivity due to translation invariance.

Keywords: Holography and condensed matter physics (AdS/CMT), Gauge-gravity correspondence

ArXiv ePrint: 1608.04653

doi:10.1007/JHEP10(2016)144

JHEP10(2016)144

Contents

1 Introduction **1**

2 Holographic superconductor on a Q-lattice **3**
2.1 Metal-insulator transition without Φ 4

3 Critical temperature and DC conductivity **4**

4 Superfluid density **7**
4.1 Holographic methods 8
4.2 Numerical results 10

5 Homes' law **12**

6 Conclusion and discussions **13**

A Equations of motion for superfluid density **14**

JHEP10(2016)144

1 Introduction

Holographic methods or gauge/gravity duality have provided novel and effective ways to analyse strongly correlated systems. In particular, there have been much effort and some successes in understanding universal properties of strongly coupled systems. Important examples include the holographic bound of the ratio of shear viscosity to entropy density (η/s) in strongly correlated plasma, linear T resistivity and Hall angle of strange metal phase [1–4].

In this paper, we study another universal property observed in high-temperature superconductors and some conventional superconductors by holographic methods. It is Home's law [5, 6], which connects three quantities in normal phase and condensed phase as follows:

$$\rho_s(T=0) = C\sigma_{\rm DC}(T_c)\,T_c\,, \tag{1.1}$$

where ρ_s is the superfluid density at zero temperature, T_c is the phase transition temperature, and $\sigma_{\rm DC}$ is the DC conductivity in the normal phase close to T_c. The point is that C is a material independent universal number. $C \approx 4.4$ for ab-plane high T_c superconductors and clean BCS superconductors or $C \approx 8.1$ for c-axis high T_c superconductors and BCS superconductors in the dirty limit. Here, ρ_s, T_c and $\sigma_{\rm DC}$ are defined to be dimensionless and the numerical values of C are computed in [7] based on the experimental data in [5, 6].

It was argued that Homes' law might be related to 'Planckian dissipation', which is the quantum limit of dissipation with the shortest possible dissipation time

$$\tau_P \sim \frac{\hbar}{k_B T}\,, \tag{1.2}$$

in the normal state of high temperature superconductors [8]. Because the η/s bound of strongly correlated plasma also can be explained by Planckian dissipation [9], Homes' law may give a good chance to find some universal physics in both condensed matter systems and quark-gluon plasma [10].

Even though the holographic models of superconductor have been extensively developed [3, 4, 11, 12] since the pioneering work by Hartnoll, Herzog, and Horowitz in 2008 [13, 14], Homes' law in this context has not been studied much. It is partly because early holographic superconductor models are translationally invariant with finite charge density.[1] As a result they cannot relax momentum and yield infinite $\sigma_{\rm DC}$ in (1.1) so C is not well defined. To have a finite $\sigma_{\rm DC}$ several methods were proposed to incorporate momentum relaxation: spatially modulated boundary conditions for bulk fields [15], massive gravity models [16], Q-lattice models [17], massless scalar models with shift symmetry [18], and models with a Bianchi VII_0 symmetry dual to helical lattices [19]. Based on these models, holographic superconductors incorporating momentum relaxation have been developed [7, 20–27].

Among the aforementioned holographic superconductors with momentum relaxation, Homes' law has been studied only in two models [7, 27]. For both cases, there are parameters representing the strength of momentum relaxation, which also can be interpreted as parameters specifying material properties. Thus, Homes' law in holographic models means that C is constant independent of momentum relaxation parameters. In [7] a holographic superconductor model in a helical lattice was analysed and Homes' law was satisfied for some restricted parameter regime. Here the amplitude and the pitch of the helix are the momentum relaxation parameters. In [27] a holographic superconductor model with massless scalar fields linear in spatial coordinate[2] are studied and Homes' law was not satisfied. Here the proportionality constant to spatial coordinate is the strength of momentum relaxation.

Therefore, it seems that Homes' law is not realized for all holographic models. Because physics behind Homes' law in [7] has not been clearly understood yet, it is important to analyse other holographic models i) to see how much holographic Homes' law is robust and ii) to find the common physical mechanism for Homes' law in different models. For this purpose, in this paper, we study Homes' law in a holographic superconductor model with Q-lattice[3] [22, 23].

We choose this model for two reasons. First, our model can be easily compared with two previous works on Homes' law: i) the model has a similar structure to the helical lattice

[1] See [10] for an early attempt for Homes' law in holographic superconductors without momentum relaxation.

[2] The property of the normal phase and superconducting phase of this model was studied in [24, 28–31] and in [23, 24] respectively.

[3] The property of the normal phase of this model was studied in [17]. See [32, 33] for a Mott system based on this model.

JHEP10(2016)144

model [7] in that it has two parameters (amplitude and wavelength of lattice) ii) the model is also similar to the massless scalar model [27] in certain limit. Second, it was argued in [7] that Homes' law might have something to do with the metal/insulator transition in normal state and it was reported that our model also has the metal-insulator transition [34].

We find that Homes' law is realized also in our Q-lattice model for certain parameter regime, similarly to the helical lattice model in [7]. However, in computing the superfluid density, there is an issue that the superfluid density is different from the charge density at zero temperature (see the end of section 4 for more details.). The same issue was also raised in other holographic superconductor models [7, 27]. To check if the superfluid density is identified correctly, we compute superfluid density in two methods: one is related to the infinite DC conductivity and the other is related to the magnetic penetration depth. Both yield the same results with finite momentum relaxation, but the only latter captures the superfluid density in the case without momentum relaxation.

This paper is organised as follows. In section 2, we introduce a holographic superconductor model with Q-lattice. The metal-insulator transition in the normal state is also reviewed. In section 3, the superconducting transition temperature and electric DC conductivity are computed. In section 4 the superfluid density is computed in two methods. In section 5 we discuss the Home's law and we conclude in section 6.

2 Holographic superconductor on a Q-lattice

In this section we briefly review a holographic superconductor model on a Q-lattice, which has been studied in detail in [22, 23]. The action is given by

$$S=\int \mathrm{d}^4x\sqrt{-g}\left[R+6-\frac{1}{4}F^2-|(\partial-iqA)\Phi|^2-m_\Phi^2\Phi\Phi^*-|\partial\Psi|^2-m_\Psi^2|\Psi|^2\right], \tag{2.1}$$

where we have chosen units such that $16\pi G=1$ and set the AdS radius to unity. The first two lines are the first holographic superconductor model [13, 14] with the U(1) gauge field A, its field strength $F=\mathrm{d}A$, and a complex scalar Φ. The last line is added to introduce momentum relaxation by assuming a specific form of Ψ as described below. To be concrete, we set the mass of two scalar fields as $m_\Psi^2=m_\Phi^2=-2$.

For classical solutions we consider the following ansatz

$$\begin{aligned}\mathrm{d}s^2&=\frac{1}{z^2}\left[-(1-z)U(z)\mathrm{d}t^2+\frac{\mathrm{d}z^2}{(1-z)U(z)}+V_1(z)\mathrm{d}x^2+V_2(z)\mathrm{d}y^2\right],\\ A&=\mu(1-z)a(z)\mathrm{d}t\,,\ \Phi=z\phi(z)\,,\Psi=e^{ikx}z\psi(z)\,,\end{aligned} \tag{2.2}$$

where U, V_1, V_2, a, ϕ and ψ are functions of only the holographic coordinate z. The holographic boundary is at $z=0$ and the black hole horizon is at $z=1$. The field theory temperature (T) is identified with the Hawking temperature $\mathrm{U}(1)/4\pi$ with the boundary condition $\mathrm{U}(0)=1$. The chemical potential (μ) in field theory corresponds to $A_t(0)$ with $a(0)=1$. The complex Φ with $m_\Phi^2=-2$ behaves as $\Phi=\varphi_1 z+\varphi_2 z^2+\cdots$ near boundary. We choose φ_1 as a source and $\varphi_2\equiv(\langle\mathcal{O}\rangle)$ as a condensate of the scalar operator. For spontaneous symmetry breaking we impose the boundary condition $\varphi_1=0$. Ψ is assumed to be

JHEP10(2016)144

the form in (2.2) which breaks translation symmetry so induces momentum relaxation. It is called Q-lattice [17]. With a choice $m_\Psi^2 = -2$ the boundary value $\psi(0) = \lambda$ corresponds to the lattice amplitude and k is the lattice wavenumber.

For $\Psi = \Phi = 0$ the system becomes the AdS-Reissner-Nordström(AdS-RN) black hole, which allows an analytic solutions: $U = 1 + z + z^2 - \mu^2 z^3/4,\ V_1 = V_2 = a = 1,\ \psi = \phi = 0$. However, for finite Φ and/or Ψ we have to resort to numerical method. Our numerical solutions may be specified by four dimensionless parameters, namely $(T/\mu, \lambda/\mu, k/\mu, q)$. To be concrete, we choose $q = 6$ and identify the holographic background dual to the field theory state at various $T/\mu \in (0, 0.4)$ for a range of $\lambda/\mu \in (0, 90)$ and $k/\mu \in (0, 20)$.

2.1 Metal-insulator transition without Φ

We are mainly interested in properties of a holographic superconductor with $\Phi \neq 0$ in this paper. However, in this subsection, let us first consider a model with $\Psi = 0$ in (2.1) to investigate the conductivity of our model without condensate. The result here will be used later to understand properties of a holographic superconductor.

For our model with $\Phi = 0$, it was shown that the DC conductivity, σ_{DC}, can be computed by horizon data [35]

$$\sigma_{\rm DC} = \left(\sqrt{\frac{V_2}{V_1}} + \frac{\mu^2 a^2 \sqrt{V_1 V_2}}{2k^2 \psi^2} \right) \Bigg|_{z=1} . \tag{2.3}$$

Plugging our numerical solutions of (2.2) into (2.3) we have computed the resistivity $\rho = 1/\sigma_{DC}$ for various values of $(T/\mu, \lambda/\mu, k/\mu)$. For example, we show the resistivity as a function of temperature for $\lambda/\mu = 50$ in figure 1. If $k/\mu = 8$ (a) the resistivity increases and if $k/\mu = 12$ (b) the resistivity decreases, as temperature lowers. Therefore, the former (a) is an insulator and the latter (b) is a metal.[4] The metal insulator transition occurs at $k/\mu \approx 10.1$. By considering several values of λ/μ and k/μ we obtained a phase diagram for metal-insulator transition (MIT), which is shown in figure 2.[5] If $k = 0$ or $\lambda = 0$ (red lines) translation symmetry is recovered and the system becomes perfect metal without momentum relaxation.

MIT can be understood also by (2.3). For small k (insulating phase), as temperature lowers it turns out $V_2(1)$ goes to zero, which yields $\sigma_{DC} \to 0$. Because the entropy of the system is $4\pi\sqrt{V_1(1)V_2(1)}$, the entropy vanishes in insulating phase. For large k (metal phase), $\psi(1)$ goes to zero similarly to figure 5, which yields a large $\sigma_{\rm DC}$. In metal phase, the entropy is finite.

3 Critical temperature and DC conductivity

To study Homes' law we need three quantities, critical temperature T_c, DC conductivity at T_c ($\sigma_{\rm DC}(T_c)$) and superfluid density. In this section we compute the first two and in the next section we investigate superfluid density in more detail.

[4] For $\Phi \neq 0$, because of a superconducting phase transition at critical temperature T_c, ρ becomes zero below T_c as shown by blue lines in figure 1.

[5] This phase diagram was first studied in [34] and here we extended the analysis for a much bigger range of λ/μ and k/μ to explore Homes' law in a big enough parameter space.

JHEP10(2016)144

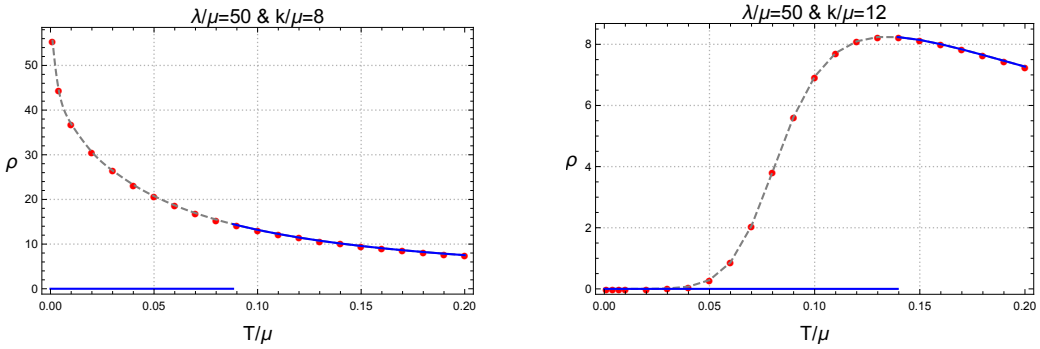

(a) Insulator. **(b)** Metal.

Figure 1. Resistivity in insulator and metal phase. Red dotted curves are the case with $\Phi = 0$. If $\Phi \neq 0$, there is a superconducting phase transition at critical temperature T_c and ρ becomes zero below T_c. It was shown as blue lines.

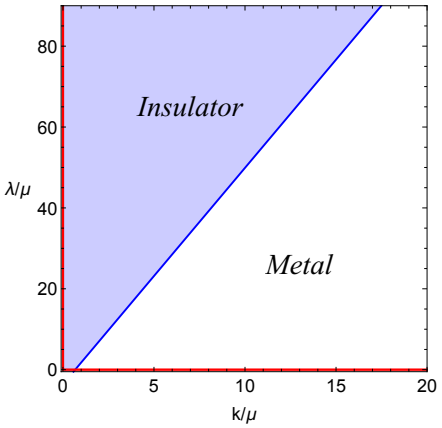

Figure 2. Metal-insulator transition with $\Phi = 0$. Red lines at $k = 0$ and $\lambda = 0$ represent perfect metals.

Using pseudo spectral method [36], we numerically constructed classical solutions (2.2) for various three dimensionless parameters $(T/\mu, \lambda/\mu, k/\mu)$ and $q = 6$. For every set of parameters $(\lambda/\mu, k/\mu)$, there is a solution with $\Phi = 0$ (normal state). In addition we find another solution with $\Phi \neq 0$ (superconducting state) below the critical temperature T_c/μ. In this case, the superconducting state has lower free energy than normal state so a phase transition occurs at T_c/μ.

In figure 3 we illustrate how the critical temperature depends on λ/μ and k/μ. First, for a fixed k/μ, the critical temperature decreases monotonically with the increase of λ/μ. Second, for a fixed λ/μ, the critical temperature first decreases for small k/μ, and then increases for large k/μ. As $k/\mu \to \infty$, it approaches to the critical temperature of the AdS-RN ($\lambda = 0$). A similar non-monotonic behaviour was also observed in the massless scalar model [24] and the helical lattice model [7]. However, this behaviour was not seen in the previous analysis of Q-lattice models [22, 23], where the scalar field Φ has a smaller charge $q = 2$ than our case ($q = 6$).

JHEP10(2016)144

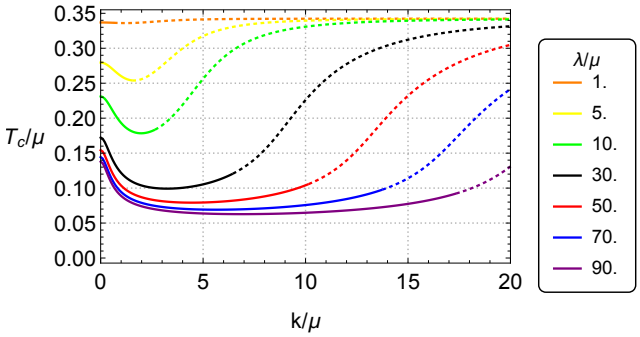

Figure 3. Critical temperature (T_c/μ) vs lattice wavenumber (k/μ) at fixed lattice amplitude ($\lambda/\mu = 1, 5, 10, 30, 50, 70, 90$). The solid part and dotted part correspond to insulator and metal respectively in figure 2.

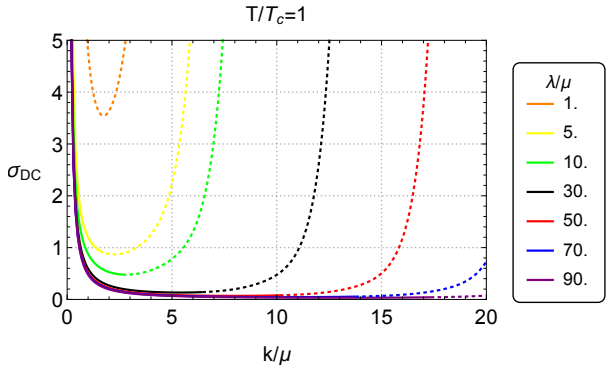

Figure 4. DC conductivity at T_c ($\sigma_{\rm DC}$) vs lattice wavenumber (k/μ) at fixed lattice amplitude ($\lambda/\mu = 1, 5, 10, 30, 50, 70, 90$). The solid part and dotted part correspond to insulator and metal respectively in figure 2.

Next, we compute the conductivity at T_c ($\sigma_{\rm DC}(T_c)$) for a range of λ/μ and k/μ. We use the formula (2.3) and our results are shown in figure 4. When $k/\mu = 0$, we have infinite $\sigma_{\rm DC}$ because the system is translationally invariant. For a fixed λ/μ, $\sigma_{\rm DC}(T_c)$ decreases when k/μ is small and increases when k/μ is large. As $k/\mu \to \infty$, it again goes to infinity.

Notice that both T_c and $\sigma_{DC}(T_c)$ approach their values of the AdS-RN as $k/\mu \to \infty$. Indeed, as shown in the following section, the superfluid density also approaches the value of the AdS-RN as $k/\mu \to \infty$. This universal feature can be understood in two ways. First, For $k/\mu \gg 1$, $\Psi = z\psi e^{ikx}$ oscillates so fast that the lattice effect is averaged out and translational symmetry is effectively restored. Second, the bulk profile of $|\Psi(z)| = z\psi$ becomes suppressed for $k/\mu \gg 1$ as shown in figure 5, where, for example, $|\Psi(z)|$ at $T/T_c = 0.1$ with $\lambda/\mu = 50$ is plotted for different k/μ. For large k/μ, $|\Psi(z)|$ are almost zero near horizon ($z = 1$) so infrared physics will not be affected by Ψ.

Figure 5 also shows that there is a qualitative change of $|\Psi(z)|$ at the critical value of $k_c/\mu \approx 10.1$. That is $|\Psi(1)| = 0$ for $k/\mu > k_c/\mu$ and $|\Psi(z)| \neq 0$ for $k/\mu < k_c/\mu$. Interestingly, this critical k_c/μ when $\Phi \neq 0$ coincides with the MIT point when $\Phi = 0$ in figure 2.

JHEP10(2016)144

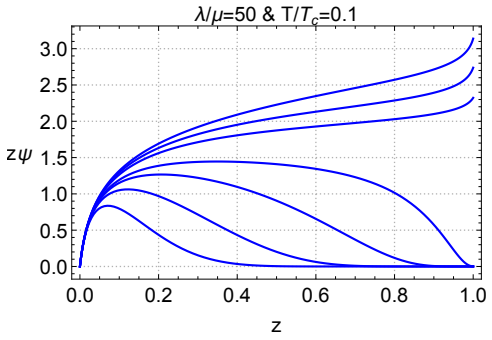

Figure 5. The bulk profile of $|\Phi| = z\psi(z)$. From top to down the curves represent $k/\mu = 2, 4, 6, 10.1, 12, 15, 20$. $T/T_c = 0.1$ and $\lambda/\mu = 50$.

In both figures 3 and 4, the curves have the solid part and the dotted part. The former has the k/μ values of insulator and the latter has the k/μ values of metal, where k/μ is read off from figure 2. It shows that k/μ dependence of T_c and $\sigma_{DC}(T_c)$ has some correlation with the MIT.

4 Superfluid density

In this section we compute the superfluid density ρ_s in two ways based on the London equation [14]:

$$J_i(\omega, \vec{p}) = -\rho_s A_i(\omega, \vec{p}) \,, \tag{4.1}$$

which is valid when ω and $\vec{p}$ are small compared to the scale at which the system loses its superconductivity. We will consider two limits: 1) $\vec{p} = 0$ and $\omega \to 0$, 2) $\omega = 0$ and $\vec{p} \to 0$. The two cases can explain the infinite DC conductivity and the Meissner effect of superconductors respectively.

First, in the limit $\vec{p} = 0$ and $\omega \to 0$, the time derivative of (4.1) gives

$$J_i(\omega, 0) = \frac{i\rho_s}{\omega} E_i(\omega, 0) \equiv \sigma(\omega) E_i(\omega, 0) \,, \tag{4.2}$$

where $\sigma(\omega)$ denotes complex optical conductivity. Thus the superfluid density is identified with the coefficient of $1/\omega$ pole in the imaginary part of the complex electric conductivity

$$\mathrm{Im}[\sigma(\omega)] = \frac{\rho_s}{\omega} + \cdots \,, \tag{4.3}$$

which implies the infinite DC conductivity (the delta function in the real part of the conductivity)

$$\mathrm{Re}[\sigma(\omega)] = \frac{\pi}{2}\rho_s \delta(\omega) \,, \tag{4.4}$$

by the Kramers-Kronig relation

$$\mathrm{Im}[\sigma(\omega)] = -\frac{2\omega}{\pi}\mathcal{P}\int_0^\infty \mathrm{d}\tilde{\omega} \frac{\mathrm{Re}[\sigma(\tilde{\omega})]}{\tilde{\omega}^2 - \omega^2} \,. \tag{4.5}$$

JHEP10(2016)144

The appearance of the delta function in $\mathrm{Re}[\sigma(\omega)]$ at $\omega = 0$ in the superconducting phase is understood as the spectral weight transferred from finite ω by the Ferrell-Glover-Tinkham (FGT) sum rule [7, 24]

$$\int_{0^+}^{\infty} \mathrm{d}\omega\, \mathrm{Re}[\sigma_n(\omega) - \sigma_s(\omega)] = \frac{\pi}{2}\rho_s\,, \tag{4.6}$$

where σ_n and σ_s denote the electric optical conductivity in the normal phase and superconducting phase respectively. Physically, it means that the charged degrees of freedom of the system are conserved.

Second, in the limit $\omega = 0$ and $\vec{p} \to 0$, the curl of (4.1) gives $\nabla \times \vec{J} = -\rho_s \vec{B}$. With Maxwell's equation $\nabla \times \vec{B} = 4\pi \vec{J}$, we have

$$\begin{aligned} -\nabla^2 \vec{B} &= \nabla \times (\nabla \times \vec{B}) \\ &= 4\pi \nabla \times \vec{J} = -4\pi \rho_s \vec{B} \equiv -\frac{1}{\lambda^2}\vec{B}\,, \end{aligned} \tag{4.7}$$

implying the Meissner effect. Here λ^2 is the magnetic penetration depth squared which is inversely proportional to the superfluid density.

4.1 Holographic methods

Based on these two limits, the superfluid density can be obtained experimentally by measuring optical conductivity or magnetic penetration depth. Corresponding to both cases there are holographic computational methods. According to the AdS/CFT correspondence A_i and J_i in (4.1) are identified with the leading term $a_i^{(0)}$ and the sub-leading term $a_i^{(1)}$ in the expansion of the bulk gauge field $a_i(z)$ near boundary $z = 0$:

$$a_i(z, \omega, \vec{p}) = a_i^{(0)}(\omega, \vec{p}) + z a_i^{(1)}(\omega, \vec{p}) + \cdots\,. \tag{4.8}$$

Thus

$$\rho_s = -\left.\frac{a_i^{(1)}(\omega, \vec{p})}{a_i^{(0)}(\omega, \vec{p})}\right|_{\{\omega, \vec{p}\} \to 0}\,. \tag{4.9}$$

We can compute this by choosing a different limit 1) $\vec{p} = 0$ and $\omega \to 0$, 2) $\omega = 0$ and $\vec{p} \to 0$ corresponding to the optical conductivity and the magnetic penetration depth respectively.[6] However, there is a subtle issue in the order of limit. The two limits $\omega \to 0$ and $\vec{p} \to 0$ may not commute. In the probe limit, it was shown that the two limits commute [4], but in the case of full back reaction as in our set-up, these two limits may not commute. Because of this potential subtlety we will introduce new notations for superfluid density: K_s for the case 1) and $\tilde{K}_s$ for the case 2).

First, to calculate the superfluid density in the limit $\vec{p} = 0$ and $\omega \to 0$, we introduce a small fluctuation of the gauge field of the form [22, 23]

$$\delta A_x = e^{-i\omega t} a_x(z)\,, \tag{4.10}$$

[6] Since the gauge field in the holographic model is external, currents do not source electromagnetic fields and Maxwell's equation can not be applied in (4.7), but we still have a London equation.

JHEP10(2016)144

which is coupled to the fluctuations of the metric and the scalar field Ψ:

$$\delta g_{tx} = e^{-i\omega t} h_{tx}(z), \quad \delta\Psi = i e^{-i\omega t} e^{ikx} z\chi(z)\,. \tag{4.11}$$

The equations of motion for $a_x(z), h_{tx}(z)$ and $\chi(z)$ are shown in appendix A. Near boundary the asymptotic behaviour of the fluctuations are as follows:

$$a_x(z) = a_x^{(0)} + z a_x^{(1)} + \cdots, \tag{4.12}$$

$$\chi(z) = \chi^{(0)} + z\chi^{(1)} + \cdots, \tag{4.13}$$

$$h_{tx}(z) = \frac{h_{tx}^{(0)}}{z^2} + \cdots. \tag{4.14}$$

We want to read off the electric conductivity only with electric field turned on, i.e. $\chi^{(0)} = h_{tx}^{(0)} = 0$ However, as explained in detail in [17] if we impose ingoing boundary conditions near horizon it turns out that the number of independent parameters becomes only two, one of which should be $a_x^{(0)}$. Thus we cannot set both $\chi^{(0)}$ and $h_{tx}^{(0)}$ to be zero. However, if we impose $\omega\chi^{(0)} - ik\lambda h_{tx}^{(0)} = 0$. we may turn off the other sources by using diffeomorphism [17]. With this condition we get

$$\rho_s = -\left.\frac{a_x^{(1)}(\omega,0)}{a_x^{(0)}(\omega,0)}\right|_{\omega\to 0} \equiv K_s\,, \tag{4.15}$$

which is equivalent to (4.2) because $i\omega a_x^{(0)}(\omega,0) = E_x$ and $a_x^{(1)}(\omega,0) = J_x$ by the AdS/CFT correspondence.

Next we study the limit $\omega = 0$ and $\vec{p} \to 0$. In this case we introduce a fluctuation in A_x that have momentum dependence of the form [37]

$$\delta A_x = e^{ipy} a_x(z)\,. \tag{4.16}$$

Unlike [37], we consider the back-reaction so δA_x is coupled to the metric fluctuation:

$$\delta g_{tx} = e^{ipy} h_{tx}(z). \tag{4.17}$$

The equations of motions for these two fluctuations are written in appendix A. Near boundary

$$a_x(z) = a_x^{(0)} + z a_x^{(1)} + \cdots, \tag{4.18}$$

$$h_{tx}(z) = \frac{h_{tx}^{(0)}}{z^2} + \cdots, \tag{4.19}$$

and setting $h_{tx}^{(0)} = 0$ we have

$$\rho_s = -\left.\frac{a_x^{(1)}(0,p)}{a_x^{(0)}(0,p)}\right|_{p\to 0} \equiv \tilde{K}_s\,. \tag{4.20}$$

JHEP10(2016)144

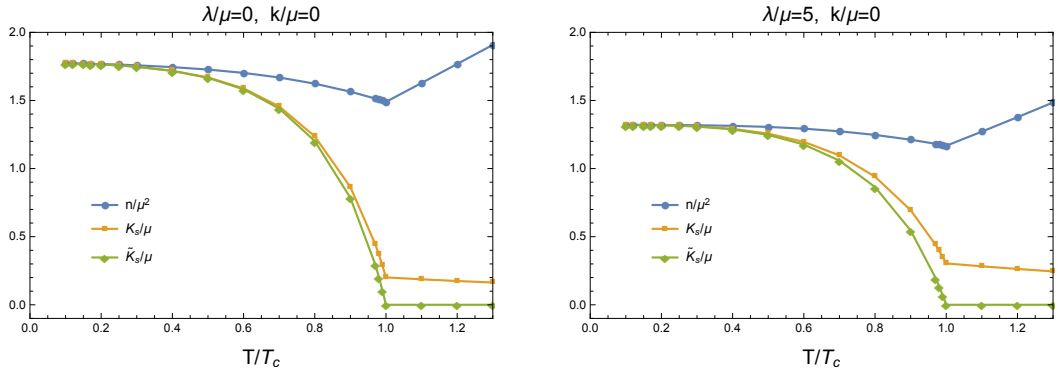

(a) No momentum relaxation. **(b)** No momentum relaxation.

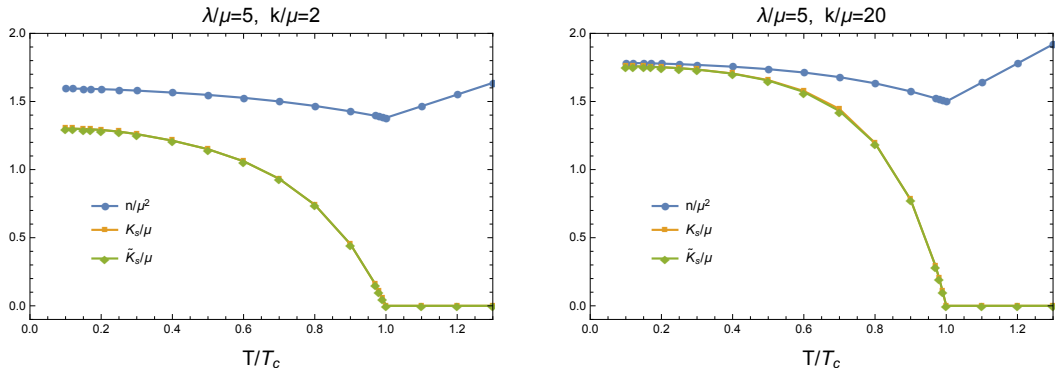

(c) Large momentum relaxation. **(d)** Small momentum relaxation.

Figure 6. The charge density n, superfluid density K_s, and $\tilde{K_s}$ vs T/T_c.

4.2 Numerical results

Using (4.15) and (4.20) we have computed K_s and $\tilde{K}_s$ as functions of T/T_c for different sets of parameters λ/μ and k/μ. For example, in figure 6, we show our results for four cases: $(\lambda/\mu, k/\mu) = (0,0), (5,0), (5,2), (5,20)$. The orange curves are for K_s/μ and the green curves are for $\tilde{K}_s/\mu$. The blue curves represent the charge density n/μ^2 ,[7] which is added for comparison.

First, we display the cases with no momentum relaxation in figure 6 (a) and (b): (a) is the case of AdS-RN geometry because $\lambda/\mu = 0$ means $\Psi(z) = 0$. (b) is not AdS-RN, since there is a finite scalar field $\Psi(z)$ with a boundary value $\psi(0)/\mu = 5$. However, the boundary theory is still translationally invariant because $k = 0$. Here we find that $K_s \neq \tilde{K}_s$ in general. We expect the superfluid density vanishes $T > T_c$ so the superfluid density should be identified with $\tilde{K}_s$. The non-zero K_s for $T > T_c$ may be interpreted as a spurious effect by the infinite DC conductivity due to translational invariance. This is an interesting and useful observation, since $\tilde{K}_s$ gives a direct way to compute the superfluid density even in the case with translation invariance.

[7] The charge density is defined by a sub-leading term of A_t in (2.2). i.e. $A_t = \mu - nz + \cdots$ near boundary.

JHEP10(2016)144

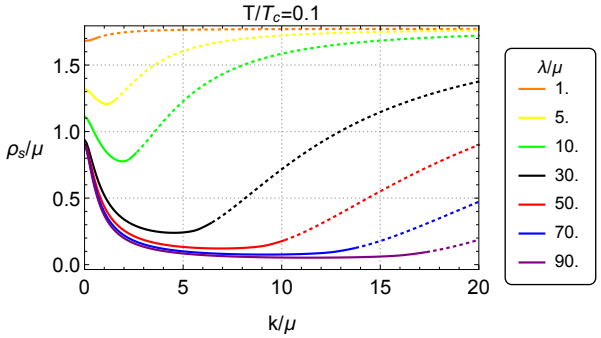

Figure 7. Superfluid density $\rho_s/\mu(= K_s/\mu = \tilde{K}_s/\mu)$ at $T/T_c = 0.1$ vs lattice wavenumber (k/μ) at fixed lattice amplitude $(\lambda/\mu = 1, 5, 10, 30, 50, 70, 90)$. The solid part and the dotted part correspond to insulator and metal respectively in figure 2.

Next, let us turn to the case with momentum relaxation in figure 6 (c) and (d). Here $K_s = \tilde{K}_s$ and they are zero for $T > T_c$, which means that the aforementioned spurious contribution to K_s by translational invariance vanishes. Notice that the superfluid density $\tilde{K}_s$ in figure 6 (d) is similar to $\tilde{K}_s$ in figure 6 (a). It is because in the limit $k \to \infty$ the translation invariance is effectively restored as explained at the end of section 3. In this limit the value of λ becomes irrelevant and the geometry approaches to the AdS-RN not the one for figure 6 (b).

For our goal (Homes' law), we need to know ρ_s at zero T. $\rho_s = K_s = \tilde{K}_s$ near zero temperature for all cases, so we will use the notation ρ_s for superfluid density. For example, ρ_s at zero T can be read from figure 6 (b),(c),(d), for $\lambda/\mu = 5$ and $k/\mu = 0, 2, 20$ respectively. Because of numerical instability of our numerical analysis we have obtained data up to $T/T_c = 0.1$ and extrapolated them to $T = 0$. We have done this analysis for a range of λ/μ and k/μ and our results are shown in figure 7. For a fixed λ/μ, ρ_s/μ at zero T decreases when k/μ is small and increases when k/μ is large. As $k/\mu \to \infty$, it approaches to the AdS-RN value regardless of λ. In the curves, the solid part has the k/μ values of insulator and the dotted part has the k/μ values of metal in figure 2. Similarly to T_c (figure 3) and $\sigma_{DC}(T_c)$ (figure 4), the k/μ dependence of the superfluid density has some correlation with the MIT.

At zero temperature, without momentum relaxation $K_s/\mu = n/\mu^2$ (figure 6(a)(b)) while with momentum relaxation $K_s/\mu \neq n/\mu^2$ (figure 6(c)). This difference was also observed in other holographic superconductor models with momentum relaxation [10, 27], so it seems a general feature of holographic superconductors. Because the FGT sum rule (4.6) still holds even with $K_s/\mu \neq n/\mu^2$ we may conclude that some of the low frequency spectral weight is transferred to finite frequencies rather than the delta function at zero frequency. As another possibility to explain $K_s/\mu \neq n/\mu^2$ at zero T [10], it was argued that the identification of superfluid density in (4.3) or (4.15) may not be correct and it was proposed to cross check it via the magnetic penetration depth, which is (4.20). We have cross checked it in our model and find two methods agree, $K_s = \tilde{K}_s$.

JHEP10(2016)144

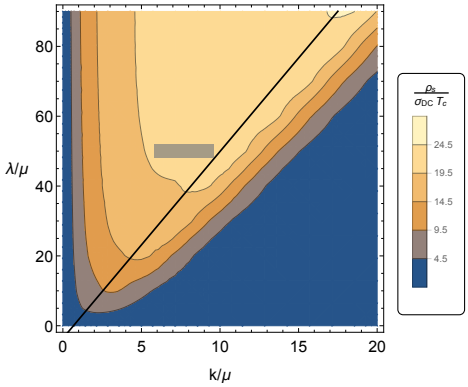

(a) Contour plot of $C = \rho_s/(\sigma_{DC}T_c)$ in λ/μ-k/μ plane.

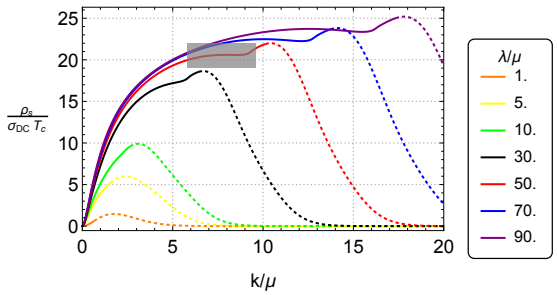

(b) Cross-sections of (a) at $\lambda/\mu = 1, 5, 10, 30, 50, 70, 90$. The solid part and the dotted part correspond to insulator and metal respectively in figure 2.

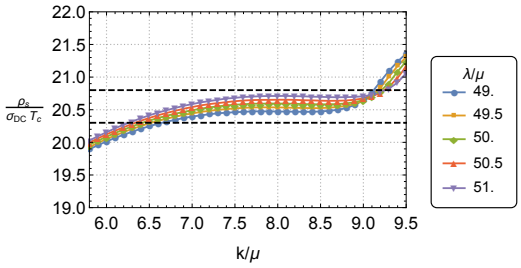

(c) Zoom-in of the grey window in (b).

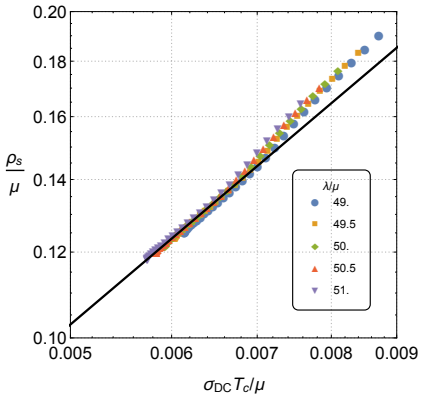

(d) ρ_s/μ vs $(\sigma_{DC}T_c/\mu)$: Log-Log plot for $\lambda/\mu \in (49, 51)$ and $k/\mu \in (7, 10)$.

Figure 8. Checking Homes' law: $C = \rho_s/(\sigma_{DC}T_c)$ as functions of $\lambda/\mu \in (0, 90)$ and $k/\mu \in (0, 20)$.

5 Homes' law

Homes' law is given by

$$\rho_s(T = 0) = C\sigma_{DC}(T_c)T_c\,, \tag{5.1}$$

where C is a universal material independent constant. In our holographic model, k and λ correspond to the properties of material so we want to check if C is constant irrespective of k and λ. Having computed T_c (figure 3), $\sigma_{DC}(T_c)$ (figure 4), and ρ_s (figure 7) as functions of k and λ we are ready to check Homes' law in our holographic superconductor model.

First, to have an overall picture, we present a contour plot of $C = \rho_s/(\sigma_{DC}T_c)$ in λ/μ-k/μ plane ($0 \leq k/\mu \leq 20$ and $0 \leq \lambda/\mu \leq 90$) in figure 8(a). The black diagonal line is the MIT line in figure 2. In general, in the region close to the MIT, C is larger and below the MIT, C becomes small quickly. C vanishes as $k/\mu \ll 1$ and $k/\mu \gg 1$ because $\sigma_{\rm DC} \gg 1$ due to the restoration of translational invariance.

JHEP10(2016)144

For $\lambda/\mu \gtrsim 40$, in a triangular region surrounded by a contour, C does not change much compared to the other region. In that region, there is a possibility that Homes' law hold. To see it more clearly we make figure 8(b), which is the cross-sections of figure 8(a) for fixed $\lambda/\mu = 1, 5, 10, 30, 50, 70, 90$. Here we can see plateaus in some range of k for every $\lambda/\mu \gtrsim 50$, which means Homes' law holds in that regime. The regime are in the insulating phase near the MIT line, which was also observed in a holographic superconductor with helical lattice [7]. In our case, Homes' law seems to hold for a wider range of λ/μ than the helical lattice case, even thought C is a little bit different for a different λ/μ.[8] In figure 8(c), we zoom in the grey window in figure 8(b) for $49 \leq \lambda/\mu \leq 51$. Figure 8 (d) is the Log-Log plot of ρ_s/μ vs $(\sigma_{DC}T_c/\mu)$ for $49 \leq \lambda/\mu \leq 51$ and $7 \leq k/\mu \leq 10$. Figure 8 (c) and (d) are similar to figure 15 in [7].

The appearance of the plateaus for large λ/μ in figure 8(b) may be qualitatively understood from figure 3, 4 and 7, where all three quantities ρ_s, $\sigma_{\rm DC}$, and T_c show the same qualitative behaviour. At fixed λ/μ, as k/μ increases, they decrease at small k/μ and reach their minimum values and again increase at large k/μ. As λ/μ grows, their minimum values are saturating and the plateaus start developing around the minimum. Bigger the λ/μ, longer the ranges of k/μ for plateaus.

However, if we look at closely, the plateau of every ρ_s, $\sigma_{\rm DC}$, ann T_c is not strictly flat. They are slightly increasing or decreasing, but the combination of them, C, shows a better plateau behaviour. To check it explicitly we have made a plot for $B \equiv \rho_s/T_c$ without $\sigma_{\rm DC}$ and found that B is not as flat as C shown in figure 8(c). Physically, this means that the Uemura's law[9] does not hold in our model.

In addition, there are also plateaus at fixed k/μ for some range of λ. It can be seen from the almost vertical part of contour lines for $k/\mu \leq 5$ in figure 8(a).

6 Conclusion and discussions

We investigated Homes' law by computing the critical temperature (T_c), the DC conductivity at the critical temperature ($\sigma_{\rm DC}(T_c)$), and the superfluid density (ρ_s) in a holographic superconductor with Q-lattice. In this set-up Homes' law means that $C = \rho_s/(T_c\sigma_{\rm DC}(T_c))$ is independent of the amplitude (λ) and/or wavenumber (k) of Q-lattice. We find that Homes' law holds for a range of k/μ at every fixed $\lambda/\mu \gtrsim 50$. As λ/μ grows, C tends to approach to some universal value. Homes' law holds in insulating phase near the metal insulator transition (MIT), where momentum relaxation is strongest. Roughly speaking, i) for a given λ/μ, there is k/μ near the MIT (say, k_c/μ) which gives the maximum value of C, ii) if λ/μ increases C becomes constant for a range of k/μ around the k_c/μ.

To compute the superfluid density, we employed two methods. One is related to the infinite DC conductivity and the other is related to the magnetic penetration depth. With finite momentum relaxation both give the same results, which serves as a good cross-check

[8] For large λ, it seems that C is approaching to the universal value. However, we could not confirm it due to numerical instability for $\lambda/\mu > 90$.

[9] Uemura's law is $\rho_s(T=0) = B\,T_c$, where B is another universal constant independent of materials. It holds only for underdoped cuprates [5, 6].

JHEP10(2016)144

of our computation. However, without momentum relaxation only the latter correctly captures the superfluid density. The former gets spurious contribution from the infinite DC conductivity due to translational invariance.

At zero temperature, with momentum relaxation $K_s/\mu \neq n/\mu^2$ while without momentum relaxation $K_s/\mu = n/\mu^2$. It was observed in other holographic models. Because the FGT sum rule (4.6) still holds it seems that some of the low frequency spectral weight is transferred to finite frequencies rather than the delta function at zero frequency.

In this paper, we considered the case with $q = 6$ and $m_\Psi^2 = -2$ in detail. We have also checked Homes' law for a different q ($q = 2$) and obtained qualitatively the same result. If m_Ψ^2 increases, it is possible that the MIT does not occur and consequently Homes' law does not hold. For example, if $m_\Psi^2 = 0$ our model becomes similar to the massless scalar model and it was shown that there is no MIT and no Homes' law in that model if Ψ does not have z dependence [27].

Homes' law in our model comes from the MIT and strong momentum relaxation. The MIT seems to be less relevant phenomenologically but strong momentum relaxation is encouraging since it is a property of incoherent metal regime where Planckian dissipation (1.2) may occur [38]. However, it turns out that our model does not have a linear in T resistivity in normal (strange metal) phase as shown in figure 1. Because the linear in T resistivity is a universal property of the normal phase of high T_c superconductors and may be related to the physics of Homes' law by the Planckian dissipation [8], it will be important to study Homes' law in a holographic model having linear in T resistivity such as [39, 40].

A Equations of motion for superfluid density

We present the equations of motion for superfluid density used in section 4. The first one is for the case $\vec{p} = 0$ and $\omega \to 0$ and the second is for $\omega = 0$ and $\vec{p} \to 0$.

1. $\vec{p} = 0$ and $\omega \to 0$

$$
\begin{aligned}
0 &= a_x'' + \left[\frac{((1-z)U)'}{(1-z)U} + \frac{1}{2}\left(\frac{V_2'}{V_2} - \frac{V_1'}{V_1}\right)\right] a_x' + \left(\frac{\omega^2}{(1-z)^2U^2} - \frac{z^2((1-z)a)'}{(1-z)U}\right) a_x \\
&\quad - \frac{2q^2\phi^2}{(1-z)U} a_x + \frac{2ikz^2((1-z)a)'(\psi'\chi - \psi\chi')}{\omega}, \\
0 &= h_{tx}' + ((1-z)a)' a_x + \left(\frac{2}{z} - \frac{V_1'}{V_1}\right) h_{tx} - \frac{2q^2\phi^2}{(1-z)U} a_x - \frac{2ik(1-z)U(\psi'\chi - \psi\chi')}{\omega}, \\
0 &= \chi'' + \left[\frac{((1-z)U)'}{(1-z)U} + \frac{1}{2}\left(\frac{V_2'}{V_2} + \frac{V_1'}{V_1}\right)\right] \chi' + \left(\frac{\omega^2}{(1-z)^2U^2} - \frac{k^2}{(1-z)UV_1}\right) \chi \\
&\quad + \frac{1}{z}\left[\frac{((1-z)U)'}{(1-z)U} + \frac{1}{2}\left(\frac{V_2'}{V_2} + \frac{V_1'}{V_1}\right)\right] \chi + \frac{2-2(1-z)U}{(1-z)z^2U} \chi - \frac{ik\omega z^2\psi}{(1-z)^2U^2V_1} h_{tx},
\end{aligned}
\tag{A.1}
$$

JHEP10(2016)144

2. $\omega = 0$ and $\vec{p} \to 0$

$$
\begin{aligned}
0 &= a_x'' + \left[\frac{((1-z)U)'}{(1-z)U} + \frac{1}{2}\left(\frac{V_2'}{V_2} - \frac{V_1'}{V_1}\right)\right] a_x' - \frac{p^2 + 2q^2 V_2 \phi^2}{(1-z)UV_2} a_x \\
&\quad + \frac{z^2((1-z)a)'}{(1-z)U} h_{tx}' + \frac{z((1-z)a)'(2V_1 - zV_1')}{(1-z)UV_1} h_{tx}, \\
0 &= h_{tx}'' + \frac{1}{2}\left(\frac{4}{z} - \frac{V_1'}{V_1} + \frac{V_2'}{V_2}\right) h_{tx}' + ((1-z)a)' a_x' + \frac{2q^2 a \phi^2}{U} a_x \\
&\quad + \left[\frac{z^2((1-z)a)'^2}{2(1-z)U} + \frac{z^4\left(\frac{(1-z)U}{z^2}\right)'\left(\frac{V_1}{z^2}\right)'}{(1-z)UV_1} - \frac{p^2 z^2 + 2V_2(3 + z^2(\psi^2 + \phi^2))}{(1-z)z^2 UV_2}\right] h_{tx}.
\end{aligned}
\tag{A.2}
$$

Acknowledgments

We would like to thank Tomas Andrade for collaborations at an early stage of this project. We also would like to thank Johanna Erdmenger, Sean Hartnoll, Elias Kiritsis, Yi Ling, Rene Meyer, Andy O'Bannon, and Koenraad Schalm for valuable discussions and correspondence. The work was supported by Basic Science Research Program through the National Research Foundation of Korea (NRF) funded by the Ministry of Science, ICT & Future Planning (NRF- 2014R1A1A1003220) and the GIST Research Institute (GRI) in 2016.

References

[1] J. Zaanen, Y.-W. Sun, Y. Liu and K. Schalm, *Holographic Duality in Condensed Matter Physics*, Cambridge University Press, Cambridge, U.K. (2015).

[2] M. Ammon and J. Erdmenger, *Gauge/gravity duality*, Cambridge University Press, Cambridge, U.K. (2015).

[3] S.A. Hartnoll, *Lectures on holographic methods for condensed matter physics*, *Class. Quant. Grav.* **26** (2009) 224002 [arXiv:0903.3246] [INSPIRE].

[4] C.P. Herzog, *Lectures on Holographic Superfluidity and Superconductivity*, *J. Phys.* **A 42** (2009) 343001 [arXiv:0904.1975] [INSPIRE].

[5] C.C. Homes, S.V. Dordevic, T. Valla and M. Strongin, *Scaling of the superfluid density in high-temperature superconductors*, *Phys. Rev.* **B 72** (2005) 134517 [cond-mat/0410719].

[6] C.C. Homes et al., *Universal scaling relation in high-temperature superconductors*, *Nature* **430** (2004) 539 [cond-mat/0404216] [INSPIRE].

[7] J. Erdmenger, B. Herwerth, S. Klug, R. Meyer and K. Schalm, *S-Wave Superconductivity in Anisotropic Holographic Insulators*, *JHEP* **05** (2015) 094 [arXiv:1501.07615] [INSPIRE].

JHEP10(2016)144

[8] J. Zaanen, *Superconductivity: Why the temperature is high*, *Nature* **430** (2004) 512.

[9] S. Sachdev and B. Keimer, *Quantum Criticality*, *Phys. Today* **64N2** (2011) 29 [arXiv:1102.4628] [INSPIRE].

[10] J. Erdmenger, P. Kerner and S. Muller, *Towards a Holographic Realization of Homes' Law*, *JHEP* **10** (2012) 021 [arXiv:1206.5305] [INSPIRE].

[11] G.T. Horowitz, *Introduction to Holographic Superconductors*, *Lect. Notes Phys.* **828** (2011) 313 [arXiv:1002.1722] [INSPIRE].

[12] R.-G. Cai, L. Li, L.-F. Li and R.-Q. Yang, *Introduction to Holographic Superconductor Models*, *Sci. China Phys. Mech. Astron.* **58** (2015) 060401 [arXiv:1502.00437] [INSPIRE].

[13] S.A. Hartnoll, C.P. Herzog and G.T. Horowitz, *Building a Holographic Superconductor*, *Phys. Rev. Lett.* **101** (2008) 031601 [arXiv:0803.3295] [INSPIRE].

[14] S.A. Hartnoll, C.P. Herzog and G.T. Horowitz, *Holographic Superconductors*, *JHEP* **12** (2008) 015 [arXiv:0810.1563] [INSPIRE].

[15] G.T. Horowitz, J.E. Santos and D. Tong, *Optical Conductivity with Holographic Lattices*, *JHEP* **07** (2012) 168 [arXiv:1204.0519] [INSPIRE].

[16] D. Vegh, *Holography without translational symmetry*, arXiv:1301.0537 [INSPIRE].

[17] A. Donos and J.P. Gauntlett, *Holographic Q-lattices*, *JHEP* **04** (2014) 040 [arXiv:1311.3292] [INSPIRE].

[18] T. Andrade and B. Withers, *A simple holographic model of momentum relaxation*, *JHEP* **05** (2014) 101 [arXiv:1311.5157] [INSPIRE].

[19] A. Donos and S.A. Hartnoll, *Interaction-driven localization in holography*, *Nature Phys.* **9** (2013) 649 [arXiv:1212.2998] [INSPIRE].

[20] G.T. Horowitz and J.E. Santos, *General Relativity and the Cuprates*, *JHEP* **06** (2013) 087 [arXiv:1302.6586] [INSPIRE].

[21] H.B. Zeng and J.-P. Wu, *Holographic superconductors from the massive gravity*, *Phys. Rev.* **D 90** (2014) 046001 [arXiv:1404.5321] [INSPIRE].

[22] Y. Ling, P. Liu, C. Niu, J.-P. Wu and Z.-Y. Xian, *Holographic Superconductor on Q-lattice*, *JHEP* **02** (2015) 059 [arXiv:1410.6761] [INSPIRE].

[23] T. Andrade and S.A. Gentle, *Relaxed superconductors*, *JHEP* **06** (2015) 140 [arXiv:1412.6521] [INSPIRE].

[24] K.-Y. Kim, K.K. Kim and M. Park, *A Simple Holographic Superconductor with Momentum Relaxation*, *JHEP* **04** (2015) 152 [arXiv:1501.00446] [INSPIRE].

[25] M. Baggioli and M. Goykhman, *Phases of holographic superconductors with broken translational symmetry*, *JHEP* **07** (2015) 035 [arXiv:1504.05561] [INSPIRE].

[26] M. Baggioli and M. Goykhman, *Under The Dome: Doped holographic superconductors with broken translational symmetry*, *JHEP* **01** (2016) 011 [arXiv:1510.06363] [INSPIRE].

[27] K.K. Kim, M. Park and K.-Y. Kim, *Ward identity and Homes' law in a holographic superconductor with momentum relaxation*, *JHEP* **10** (2016) 041 [arXiv:1604.06205] [INSPIRE].

[28] K.-Y. Kim, K.K. Kim, Y. Seo and S.-J. Sin, *Coherent/incoherent metal transition in a holographic model*, *JHEP* **12** (2014) 170 [arXiv:1409.8346] [INSPIRE].

JHEP10(2016)144

[29] K.-Y. Kim, K.K. Kim, Y. Seo and S.-J. Sin, *Gauge Invariance and Holographic Renormalization*, *Phys. Lett.* **B 749** (2015) 108 [arXiv:1502.02100] [INSPIRE].

[30] K.-Y. Kim, K.K. Kim, Y. Seo and S.-J. Sin, *Thermoelectric Conductivities at Finite Magnetic Field and the Nernst Effect*, *JHEP* **07** (2015) 027 [arXiv:1502.05386] [INSPIRE].

[31] Y. Seo, K.-Y. Kim, K.K. Kim and S.-J. Sin, *Character of matter in holography: Spin-orbit interaction*, *Phys. Lett.* **B 759** (2016) 104 [arXiv:1512.08916] [INSPIRE].

[32] Y. Ling, P. Liu, C. Niu, J.-P. Wu and Z.-Y. Xian, *Holographic fermionic system with dipole coupling on Q-lattice*, *JHEP* **12** (2014) 149 [arXiv:1410.7323] [INSPIRE].

[33] Y. Ling, P. Liu, C. Niu and J.-P. Wu, *Building a doped Mott system by holography*, *Phys. Rev.* **D 92** (2015) 086003 [arXiv:1507.02514] [INSPIRE].

[34] Y. Ling, P. Liu, C. Niu, J.-P. Wu and Z.-Y. Xian, *Holographic Entanglement Entropy Close to Quantum Phase Transitions*, *JHEP* **04** (2016) 114 [arXiv:1502.03661] [INSPIRE].

[35] A. Donos and J.P. Gauntlett, *Novel metals and insulators from holography*, *JHEP* **06** (2014) 007 [arXiv:1401.5077] [INSPIRE].

[36] M. Guo, C. Niu, Y. Tian and H. Zhang, *Applied AdS/CFT with Numerics*, PoS(Modave2015)003 [arXiv:1601.00257] [INSPIRE].

[37] K. Maeda and T. Okamura, *Characteristic length of an AdS/CFT superconductor*, *Phys. Rev.* **D 78** (2008) 106006 [arXiv:0809.3079] [INSPIRE].

[38] S.A. Hartnoll, *Theory of universal incoherent metallic transport*, *Nature Phys.* **11** (2015) 54 [arXiv:1405.3651] [INSPIRE].

[39] R.A. Davison, K. Schalm and J. Zaanen, *Holographic duality and the resistivity of strange metals*, *Phys. Rev.* **B 89** (2014) 245116 [arXiv:1311.2451] [INSPIRE].

[40] H.-S. Jung, K.-Y. Kim and C. Niu, work in progress.

JHEP10(2016)144